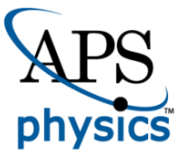

Entangling two oscillators with arbitrary asymmetric initial states

Chui-Ping Yang, Qi-Ping Su, Shi-Biao Zheng, Franco Nori, and Siyuan Han

Phys. Rev. A **95**, 052341 — Published 23 May 2017

DOI: 10.1103/PhysRevA.95.052341

Entangling two oscillators with arbitrary asymmetric initial states

Chui-Ping Yang[1], Qi-Ping Su[1], Shi-Biao Zheng[2], Franco Nori[3,4],* and Siyuan Han[5]†
[1] *Department of Physics, Hangzhou Normal University, Hangzhou, Zhejiang 310036, China*
[2] *Department of Physics, Fuzhou University, Fuzhou 350002, China*
[3] *CEMS, RIKEN, Saitama 351-0198, Japan*
[4] *Department of Physics, University of Michigan, Ann Arbor, Michigan 48109-1040, USA and*
[5] *Department of Physics and Astronomy, University of Kansas, Lawrence, Kansas 66045, USA*
(Dated: May 2, 2017)

We present a Hamiltonian, which can be used to convert any asymmetric state $|\varphi\rangle_a|\phi\rangle_b$ of two oscillators a and b into an entangled state via a single-step operation. Furthermore, with this Hamiltonian and local operations only, two oscillators, initially in any asymmetric initial states, can be entangled with a third oscillator. The prepared entangled states can be engineered with an arbitrary degree of entanglement. A discussion on the realization of this Hamiltonian is given. Numerical simulations show that, with current circuit QED technology, it is feasible to generate high-fidelity entangled states of two microwave optical fields, such as entangled coherent states, entangled squeezed states, entangled coherent-squeezed states, and entangled cat states. Our finding opens a new avenue for creating not only wave-like or particle-like entanglement but also novel wave-like and particle-like hybrid entanglement.

PACS numbers: 03.67.Bg, 42.50.Dv, 85.25.Cp

Introduction. Entangled states of light are a fundamental resource for many quantum information tasks [1-8]. In the regime of discrete variables, entanglement of up to eight photons has been experimentally demonstrated via linear optical devices [9,10]. In the regime of continuous variables, EPR states of light have been experimentally generated from two independent squeezed fields [11,12], two independent coherent fields [13], or a single squeezed light source [14]; two- or three-color entangled states of light have been experimentally prepared by means of non-degenerate optical parametric oscillators [15-17]. Recently, hybrid entanglement between particle-like and wave-like optical qubits or between quantum and classical states of light [18,19] has also been demonstrated in experiments, which has drawn increasing attention because hybrid entanglement of light is a key resource in establishing hybrid quantum networks and connecting quantum processors with different encoding qubits. Moreover, a large number of theoretical proposals have been presented for generating *particular types* of entangled states of light or photons in various physical systems [20-33].

In this paper, we propose a Hamiltonian, which can be used to convert any asymmetric state $|\varphi\rangle_a|\phi\rangle_b$ of two oscillators a and b into an entangled state $\alpha|\varphi\rangle_a|\phi\rangle_b \pm \beta|\phi\rangle_a|\varphi\rangle_b$. Here the term asymmetric state refers to the product state $|\varphi\rangle_a|\phi\rangle_b$, with $|\varphi\rangle \neq |\phi\rangle$. The procedure consists of *a single unitary operation* and a posterior measurement on the states of the qudit coupler that is used to couple the oscillators. Furthermore, by combining this Hamiltonian with additional local operations, two oscillators a and b initially in any asymmetric state $|\varphi\rangle_a|\phi\rangle_b$ and a third oscillator in the vacuum state $|0\rangle_c$ can be converted to a tripartite entangled state $\alpha|\varphi\rangle_a|\phi\rangle_b|0\rangle_c + \beta|\phi\rangle_a|\varphi\rangle_b|1\rangle_c$ with no measurement required. Hereafter, we call them the bipartite and tripartite protocols respectively. In both cases, the degree of entanglement, determined by the two coefficients α and β, is adjustable by controlling the initial state of the qudit coupler. More importantly, the light fields involved can be wave-like entangled states, particle-like entangled states, or wave-like and particle-like hybrid entangled states, depending on whether the states $|\varphi\rangle$ and $|\phi\rangle$ are both wave-like states (e.g., coherent states, squeezed states, and cat states), particle-like states (e.g., Fock states), or one wave-like and the other particle-like states (e.g., coherent states and Fock states).

Independent of the nature of the two non-identical states $|\varphi\rangle$ and $|\phi\rangle$, the bipartite protocol requires post-selection by measurement while the tripartite protocol does not. So they are not the "same". The protocol can be applied to optical cavities, microwave resonators, nano-mechanical oscillators and even hybrids of these systems. Mechanical oscillators preserve their ability to interact with almost anything and can be utilized for preparing nonclassical states of light [34-36] or matter [37]. In recent years, optical and microwave cavities/resonators as well as mechanical oscillators are playing crucial roles in quantum information processing and manipulating light or microwave photons. In fact, hybrid quantum systems have become one of the most exciting area of quantum science and technology [38].

As shown below, the entanglement generation operates essentially via the quantum state swapping conditioned on the state of the coupler. Namely, when the coupler is in the state $|g'\rangle$, the two-oscillator initial state $|\varphi\rangle_a|\phi\rangle_b$ remains unchanged; however, when the coupler is in the state $|g\rangle$, the two-oscillator initial state $|\varphi\rangle_a|\phi\rangle_b$ changes to $|\phi\rangle_a|\varphi\rangle_b$ via the state swapping $|\varphi\rangle \leftrightarrow |\phi\rangle$. Hence, the

* fnori@riken.jp
† han@ku.edu

physical mechanism used for the entanglement creation here is quite different from those based on state synthesis algorithms [39-43].

The previous protocols for entangling two oscillators in high-dimension Hilbert space are based on complex state synthesis algorithms that require a sequence of unitary operations [39-43]. In stark contrast, the present proposal requires only a single unitary operation, significantly simplifying the experimental implementation, and reducing the operation time and thus the negative effect of decoherence on fidelity. According to [35-39], the number of operations, required by state-synthesis algorithms for preparing the target states $|\Psi\rangle_{\text{target}} = \sum_{m,n} C_{mn} |m,n\rangle$, increases drastically with the dimensionality of the subspace of the Fock-state space in which the target states are embedded [39-43].

Interestingly, it is also noted that based on the proposed Hamiltonian, a SWAP gate of two *discrete-variable* qubits or two *continuous-variable* qubits can be realized in a single operation, including the two-qubit SWAP gate with *cat-state* encoding qubits which attract increasing attention recently [44].

Hamiltonian and intuition. Two oscillators a and b are coupled to a coupler with an energy level $|g\rangle$. In the interaction picture, the Hamiltonian considered here is given by (assuming $\hbar = 1$)

$$H = \omega \left(\hat{a}^\dagger \hat{a} + \hat{b}^\dagger \hat{b}\right) |g\rangle \langle g| + \lambda \left(\hat{a}^\dagger \hat{b} + \hat{a}\hat{b}^\dagger\right) |g\rangle \langle g| , \quad (1)$$

where a (b) is the photon annihilation operator of oscillator a (b), $|\omega|$ (ω being either positive or negative) is the frequency or frequency shift of both oscillators, and $|\lambda|$ (λ being either positive or negative) is the coupling strength between the two oscillators. The second term $\lambda \left(\hat{a}^\dagger \hat{b} + \hat{a}\hat{b}^\dagger\right) |g\rangle \langle g|$ represents the interaction between the two oscillators when the coupler is in the state $|g\rangle$. After some interaction time, this term results in the exchange of the states of the two oscillators when the coupler is in the state $|g\rangle$. However, the two-oscillator state exchange is imperfect without including the first term $\omega \left(\hat{a}^\dagger \hat{a} + \hat{b}^\dagger \hat{b}\right) |g\rangle \langle g|$, because the state exchange resulting from the second term $\lambda \left(\hat{a}^\dagger \hat{b} + \hat{a}\hat{b}^\dagger\right) |g\rangle \langle g|$ comes with inevitable photon-number-dependent phase errors. For instance, the state $|\varphi\rangle = \sum_{n=0}^{\infty} c_n |n\rangle$ of oscillator a (with $|n\rangle$ being the n-photon Fock state) is transferred onto oscillator b initially in a vacuum state by an error state $|\varphi\rangle_{\text{er}} = \sum_{n=0}^{\infty} c_n e^{i\phi_n} |n\rangle$ (see the discussion below).

Note that Eq. (1) is different from the well-known Hamiltonian $\widetilde{H} = \omega \left(\hat{a}^\dagger \hat{a} + \hat{b}^\dagger \hat{b}\right) + \lambda \left(\hat{a}^\dagger \hat{b} + \hat{a}\hat{b}^\dagger\right)$ describing two single-mode interacting oscillators. This is because each term in Eq. (1) contains a coupler operator $|g\rangle \langle g|$, which is however not involved in $\widetilde{H}$.

Entangling oscillators. Suppose that oscillator a is in an arbitrary pure state $|\varphi\rangle_a$ and oscillator b is in another arbitrary pure state $|\phi\rangle_b$. Assume that a coupler is in a superposition state $\alpha |g'\rangle + \beta |g\rangle$, with $|\alpha|^2 + |\beta|^2 = 1$. Here, $|g'\rangle$ is an excited state of the coupler. Under the Hamiltonian in Eq. (1), the initial state of the system $|\varphi\rangle_a |\phi\rangle_b (\alpha |g'\rangle + \beta |g\rangle)$ evolves into

$$\begin{aligned} & e^{-iHt} |\varphi\rangle_a |\phi\rangle_b (\alpha |g'\rangle + \beta |g\rangle) \\ & = \alpha |\varphi\rangle_a |\phi\rangle_b |g'\rangle + \beta \left(e^{-iH_e t} |\varphi\rangle_a |\phi\rangle_b\right) \otimes |g\rangle , \end{aligned} \quad (2)$$

where we have used $\langle g | g'\rangle = 0$. Here, $H_e = H_0 + H_I$ with $H_0 = \omega \left(\hat{a}^\dagger \hat{a} + \hat{b}^\dagger \hat{b}\right)$ and $H_I = \lambda \left(\hat{a}^\dagger \hat{b} + \hat{a}\hat{b}^\dagger\right)$. H_e describes the dynamics of the oscillators, which arises from Eq. (1) when the coupler is in the state $|g\rangle$. Because of $[H_0, H_I] = 0$, the oscillator state $e^{-iH_e t} |\varphi\rangle_a |\phi\rangle_b$ of Eq. (2) can be written as

$$e^{-iH_e t} |\varphi\rangle_a |\phi\rangle_b = U_2 U_1 |\varphi\rangle_a |\phi\rangle_b , \quad (3)$$

with $U_1 = e^{-iH_I t}$ and $U_2 = e^{-iH_0 t}$.

U_1 leads to the transformations $U_1 \hat{a}^\dagger U_1^+ = \cos(\lambda t)\hat{a}^\dagger - i \sin(\lambda t)\hat{b}^\dagger$ and $U_1 \hat{b}^\dagger U_1^+ = \cos(\lambda t)\hat{b}^\dagger - i \sin(\lambda t)\hat{a}^\dagger$. For $|\lambda| t = (2m + 1/2)\pi$ (m is an integer), one has $U_1 \left(\hat{a}^\dagger\right)^n U_1^+ = \left(\mp i \hat{b}^\dagger\right)^n$ and $U_1 \left(\hat{b}^\dagger\right)^n U_1^+ = \left(\mp i \hat{a}^\dagger\right)^n$, which will be applied in derivation of Eq. (5) below. Here and below, the sign "$-$" corresponds to $\lambda > 0$ while "$+$" corresponds to $\lambda < 0$. The arbitrary pure states $|\varphi\rangle_a$ and $|\phi\rangle_b$ can be expressed as

$$|\varphi\rangle_a = \sum_{n=0}^{\infty} c_n |n\rangle_a , \quad |\phi\rangle_b = \sum_{m=0}^{\infty} d_m |m\rangle_b , \quad (4)$$

where c_n and d_m are normalized coefficients, $|n\rangle_a = \frac{\left(\hat{a}^\dagger\right)^n}{\sqrt{n!}} |0\rangle_a$ ($|m\rangle_b = \frac{\left(\hat{b}^\dagger\right)^m}{\sqrt{m!}} |0\rangle_b$) representing the n-photon (m-photon) Fock state of oscillator a (b).

By performing a unitary transformation U_1, after $t = \pi / (2|\lambda|)$, the state $|\varphi\rangle_a |\phi\rangle_b$ evolves into

$$\begin{aligned} & U_1 |\varphi\rangle_a |\phi\rangle_b \\ & = \sum_{n=0}^{\infty} \sum_{m=0}^{\infty} \frac{c_n d_m}{\sqrt{n!m!}} \left[U_1 \left(\hat{a}^\dagger\right)^n U_1^+\right] \left[U_1 \left(\hat{b}^\dagger\right)^m U_1^+\right] U_1 |0\rangle_a |0\rangle_b \\ & = \sum_{n=0}^{\infty} c_n (\mp i)^n \frac{\left(\hat{b}^\dagger\right)^n}{\sqrt{n!}} |0\rangle_a \times \sum_{m=0}^{\infty} d_m (\mp i)^m \frac{\left(\hat{a}^\dagger\right)^m}{\sqrt{m!}} |0\rangle_b \\ & = \sum_{n=0}^{\infty} c_n e^{\mp i n\pi/2} |n\rangle_b \otimes \sum_{m=0}^{\infty} d_m e^{\mp i m\pi/2} |m\rangle_a , \end{aligned} \quad (5)$$

where the positions of $|0\rangle_a$ and $|0\rangle_b$ in line 3 are exchanged in the last line and $U_1 |0\rangle_a |0\rangle_b = |0\rangle_a |0\rangle_b$ is applied. The first (second) part of the product in the last line represents the state of oscillator b (a). Comparing the last line with the original states $|\varphi\rangle_a$ and $|\phi\rangle_b$ given in Eq. (4), one can see that the two oscillators exchange their states while accumulating photon-number-dependent phase errors $e^{\mp i n\pi/2}$ and $e^{\mp i m\pi/2}$, respectively.

By performing a unitary transformation U_2 with $t = \pi/(2|\lambda|)$ and setting $\mp\pi/2 - \omega t = 2k\pi$ (k is an integer), the state (5) becomes

$$\begin{aligned} & U_2\left(U_1|\varphi\rangle_a|\phi\rangle_b\right) \\ &= \sum_{n=0}^{\infty} c_n e^{in(\mp\pi/2-\omega t)}|n\rangle_b \otimes \sum_{m=0}^{\infty} d_m e^{im(\mp\pi/2-\omega t)}|m\rangle_a \\ &= \sum_{n=0}^{\infty} c_n|n\rangle_b \otimes \sum_{m=0}^{\infty} d_m|m\rangle_a = |\varphi\rangle_b|\phi\rangle_a, \end{aligned} \tag{6}$$

where $|\varphi\rangle_b$ ($|\phi\rangle_a$) takes the same form of the state $|\varphi\rangle_a$ ($|\phi\rangle_b$) with the subscript a (b) replaced by b (a). Combining Eqs. (3) and (6), one finds that the state (2) would be

$$\alpha|\varphi\rangle_a|\phi\rangle_b|g'\rangle + \beta|\phi\rangle_a|\varphi\rangle_b|g\rangle. \tag{7}$$

Now apply a classical pulse to the coupler, resulting in $|g'\rangle \to (|g\rangle + |g'\rangle)/\sqrt{2}$ and $|g\rangle \to (|g\rangle - |g'\rangle)/\sqrt{2}$. Thus, the state (7) becomes

$$\frac{1}{\sqrt{2}}\left(|\psi^+\rangle \otimes |g\rangle + |\psi^-\rangle \otimes |g'\rangle\right), \tag{8}$$

with

$$|\psi^{\pm}\rangle = \alpha|\varphi\rangle_a|\phi\rangle_b \pm \beta|\phi\rangle_a|\varphi\rangle_b. \tag{9}$$

Eq. (8) shows that when the coupler is measured in the state $|g\rangle$ ($|g'\rangle$), the two oscillators are prepared in an entangled state $|\psi\rangle^+$ ($|\psi^-\rangle$), for which the degree of entanglement can be adjusted by varying α and β during the preparation of the initial state of the coupler.

It is straightforward to show that the state (7) can be transformed to a three-oscillator entangled state

$$\alpha|\varphi\rangle_a|\phi\rangle_b|1\rangle_c + \beta|\phi\rangle_a|\varphi\rangle_b|0\rangle_c, \tag{10}$$

by performing local operations on the coupler and a third oscillator c initially in the vacuum state. For instance, this transformation from the state (7) to the state (10) can be achieved by tuning the frequency of oscillator c on resonance with the $|g\rangle \leftrightarrow |g'\rangle$ transition or vice versa, to have a single photon emitted into oscillator c when the coupler is in the excited state $|g'\rangle$.

Hamiltonian construction. The four levels of the coupler are denoted as $|g\rangle$, $|g'\rangle$, $|e\rangle$, and $|f\rangle$ [Fig. 1(a)]. The level $|g'\rangle$ can remain unaffected, for example, by having the transition between $|g'\rangle$ and any other level highly detuned from the frequencies of the two oscillators and the classical pulse. Oscillator a (b) is coupled to the $|g\rangle \leftrightarrow |f\rangle$ ($|g\rangle \leftrightarrow |e\rangle$) transition with coupling strength g_a (g_b) and detuning $\Delta_a = \omega_{fg} - \omega_a$ ($\delta_b = \omega_{eg} - \omega_b$) [Fig. 1(a)]. Here, ω_{fg} (ω_{eg}) is the $|g\rangle \leftrightarrow |f\rangle$ ($|g\rangle \leftrightarrow |e\rangle$) transition frequency and ω_a (ω_b) is the frequency of oscillator a (b). A classical pulse of frequency ω_p is coupled to the $|e\rangle \leftrightarrow |f\rangle$ transition with detunings $\Delta = \omega_{fe} - \omega_p$ [Fig. 1(a)]. In the interaction picture under the free Hamiltonian $H_{\rm field} + H_{\rm atom}$ with $H_{\rm field} = \omega_a\hat{a}^\dagger\hat{a} + \omega_b\hat{b}^\dagger\hat{b}$, the Hamiltonian is given by

$$\begin{aligned} H = & \left(g_a e^{i\Delta_a t}\hat{a}\sigma_{fg}^+ + g_b e^{i\delta_b t}\hat{b}\sigma_{eg}^+ + \text{H.c.}\right) \\ & + \left(\Omega e^{i\Delta t}\sigma_{fe}^+ + \text{H.c.}\right), \end{aligned} \tag{11}$$

where $\sigma_{fg}^+ = |f\rangle\langle g|$, $\sigma_{fe}^+ = |f\rangle\langle e|$, Ω is the Rabi frequency of the classical pulse, and $\hat{a}$ ($\hat{b}$) is the photon annihilation operator of oscillator a (b).

Under large-detuning conditions and when the levels $|e\rangle$ and $|f\rangle$ are not occupied, the Hamiltonian of Eq. (11) can be expressed as the following effective Hamiltonian (see Appendix)

$$\begin{aligned} H_{\rm eff} = & -\left(g_a^2/\Delta_a + \widetilde{g}_a^2/\delta\right)\hat{a}^\dagger\hat{a}|g\rangle\langle g| - g_b^2/\delta\hat{b}^\dagger\hat{b}|g\rangle\langle g| \\ & + \lambda\left(\hat{a}\hat{b}^\dagger + \hat{a}^\dagger\hat{b}\right)|g\rangle\langle g|, \end{aligned} \tag{12}$$

where $\tilde{g}_a = g_a\Omega(\Delta_a^{-1} + \Delta^{-1})/2$, $\delta_a = \Delta_a - \Delta$, and $\lambda = \widetilde{g}_a g_b/\delta > 0$. In Eq. (12), we have set $\delta_a = \delta_b \equiv \delta > 0$, i.e., $\omega_p = \omega_a - \omega_b$, which can be readily achieved by adjusting the pulse frequency ω_p. By setting

$$\frac{g_a^2}{\Delta_a} + \frac{g_a^2\Omega^2}{4\delta}\left(\Delta_a^{-1} + \Delta^{-1}\right)^2 = \frac{g_b^2}{\delta} = -\omega, \tag{13}$$

(e.g., by adjusting the pulse Rabi frequency Ω), one sees that Eq. (12) takes the same form as the Hamiltonian (1). Based on Eq. (13) and setting $\mp\pi/2 - \omega t = 2k\pi$, we can obtain the following relationship between the various parameters

$$\begin{aligned} g_b &= \frac{|4k \pm 1|}{2\sqrt{2k(2k \pm 1)\Delta_a/\delta}} g_a, \\ \Omega &= \frac{\Delta\Delta_a}{\Delta + \Delta_a}\sqrt{\delta/[2k(2k \pm 1)\Delta_a]}, \end{aligned} \tag{14}$$

which shows that the pulse Rabi frequency Ω is independent of the coupling strengths g_a and g_b.

Note that the four-level structure in Fig. 1(a) is widely available in natural or artificial atoms such as quantum dots, NV centers, and various superconducting devices [45]. Thus, the Hamiltonian (1) can be realized with a variety of physical systems. As shown above, the Hamiltonian (12), i.e., Eq. (1), was constructed based on the Raman transition induced by the field-pulse cooperation. Note that it is possible to construct the proposed Hamiltonian (1) based on other physical mechanisms.

Circuit-QED Implementation. Circuit QED with resonators and superconducting qubits is one of the most promising candidates for quantum information processing (for reviews, see [46-49]). We now consider a setup consisting of two microwave resonators coupled via a superconducting artificial atom [Fig. 1(b)]. Each resonator here is a 1D transmission line resonator (TLR). The four levels of the coupler are illustrated in Fig. 1(a). The pulse- or resonator-induced unwanted transitions between irrelevant levels are assumed to be negligibly small. This can be achieved by a prior design of the coupler with

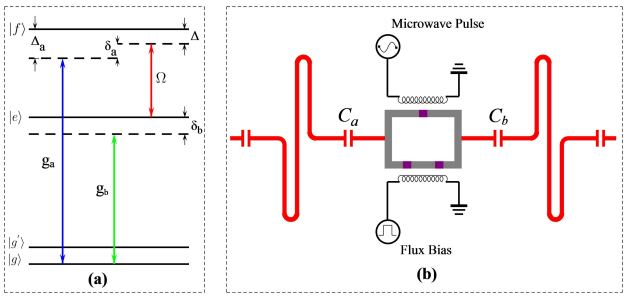

FIG. 1. (color online). (a). Illustration of the coupler interacting with two oscillators and a classical pulse. Here, $\delta_a = \omega_p + \omega_{eg} - \omega_a = \delta_b$, which can be readily met by adjusting the pulse frequency ω_p. (b). Set-up of two cavities coupled to a flux device via a capacitor C_a or C_b.

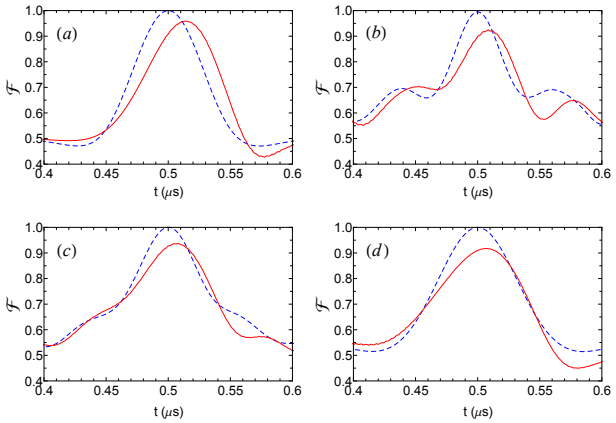

FIG. 2. (color online). Fidelities versus the operation time t. (a), (b), (c), and (d) are for entangled coherent states, entangled squeezed states, entangled coherent-squeezed states, and entangled cat states, respectively. Dashed-blue curves were based on the effective Hamiltonian (12) without considering decoherence; while red curves were based on the master equation (15) by taking decoherence into consideration.

a strong anharmonicity (e.g., a superconducting flux device). Alternatively, this condition can be satisfied by adjusting the coupler level spacings or the resonator frequencies. In practice, level spacings of superconducting devices can be rapidly adjusted within a few nanoseconds (e.g., see [50] and references therein) and, to a lesser extent, frequencies of the resonators can be fast tuned in 1-3 ns [51,52]. When the inter-resonator crosstalk is taken into account, the Hamiltonian (11) becomes $H' = H + \varepsilon$, where ε describes the unwanted inter-resonator crosstalk, given by $\varepsilon = g_{ab} e^{i\Delta_{ab}t} \hat{a}^\dagger \hat{b} + h.c.$, with the two-resonator coupling strength g_{ab} and the resonator frequency detuning $\Delta_{ab} = \omega_a - \omega_b$. Here, ω_a (ω_b) is the frequency of resonator a (b).

The fidelity of the operation is given by $\mathcal{F} = \sqrt{\langle\psi_{id}|\,\rho\,|\psi_{id}\rangle}$, where $|\psi_{id}\rangle$ is the ideal state given in Eq. (7), while ρ is the final density operator of the whole system after the operation is performed in a realistic system. As an example, we consider $\alpha = \beta = 1/\sqrt{2}$.

By solving the master equation and choosing the system parameters appropriately (see Supplemental Material), the simulated fidelity $\mathcal{F}$ versus the operation time t are shown in Fig. 2 for $\eta = \Delta_a/g_a = 25$, $k = 1$ and $\alpha = \xi = 1$, where $|\pm\xi\rangle$ are squeezed vacuum states. One can see that for $t \sim 0.5$ μs, a high fidelity can be obtained: (i) $\mathcal{F} \simeq 0.959$ for the entangled coherent states $\frac{1}{\sqrt{2}}(|\alpha\rangle_a|-\alpha\rangle_b \pm |-\alpha\rangle_a|\alpha\rangle_b)$ [Fig. 2(a)]; (ii) $\mathcal{F} \simeq 0.912$ for the entangled squeezed states $\frac{1}{\sqrt{2}}(|\xi\rangle_a|-\xi\rangle_b \pm |-\xi\rangle_a|\xi\rangle_b)$ [Fig. 2(b)]; (iii) $\mathcal{F} \simeq 0.929$ for the entangled coherent-squeezed states $\frac{1}{\sqrt{2}}(|\alpha\rangle_a|\xi\rangle_b \pm |\xi\rangle_a|\alpha\rangle_b)$ [Fig. 2(c)]; and (iv) $\mathcal{F} \simeq 0.918$ for the entangled cat states $\frac{1}{\sqrt{2}}(|\text{cat}\rangle_a|\overline{\text{cat}}\rangle_b \pm |\overline{\text{cat}}\rangle_a|\text{cat}\rangle_b)$.

For $\eta = 25$, we have $g_a/2\pi \sim 60$ MHz, $g_b/2\pi \sim 25$ MHz, and $\Omega/2\pi \sim 114$ MHz, which are available in experiments [53,54]. The frequency of a circuit resonator is typically a few GHz. For the sake of concreteness, consider $\omega_a/(2\pi) \sim 7.5$ GHz and $\omega_b/(2\pi) \sim 4.5$ GHz. For the values of κ_a^{-1} and κ_b^{-1} used in the numerical simulation, the required quality factors for the two resonators are $Q_a \sim 9.4 \times 10^5$ and $Q_b \sim 5.6 \times 10^5$, readily available in experiments [55,56]. The analysis here demonstrates that by applying the proposed protocol, the high-fidelity generation of entanglement between asymmetric states of two oscillators is feasible with current circuit QED technology. Finally, we remark that the fidelity obtained above was calculated without considering the initial state preparation and measurement errors, which however could be negligible due to progress in accurate preparation and measurement of the states of superconducting artificial atoms [57].

Finally, it is noted that based on the Hamiltonian (1), when the coupler is in the state $|g\rangle$, a SWAP gate of two *discrete-variable* qubits or two *continuous-variable* qubits, defined by $|\varphi\rangle_a|\varphi\rangle_b \to |\varphi\rangle_a|\varphi\rangle_b$, $|\varphi\rangle_a|\phi\rangle_b \to |\phi\rangle_a|\varphi\rangle_b$, $|\phi\rangle_a|\varphi\rangle_b \to |\varphi\rangle_a|\phi\rangle_b$, and $|\phi\rangle_a|\phi\rangle_b \to |\phi\rangle_a|\phi\rangle_b$, can be realized via a single operation. Here, a qubit is encoded by the two states $|\varphi\rangle$ and $|\phi\rangle$ of each oscillator. For $|\varphi\rangle = |\text{cat}\rangle$ and $|\phi\rangle = |\overline{\text{cat}}\rangle$, the two-qubit SWAP gate is implemented with *cat-state* encoding qubits [44].

Acknowledgments. C.P.Y. and Q.P.S. were supported in part by the Ministry of Science and Technology of China under Grant No. 2016YFA0301802, the National Natural Science Foundation of China under Grant Nos. [11074062, 11374083, 11504075], and the Zhejiang Natural Science Foundation under Grant No. LZ13A040002. S.B.Z. was supported by the Major State Basic Research Development Program of China under Grant No. 2012CB921601. F.N. was supported by the RIKEN iTHES Project, the MURI Center for Dynamic Magneto-Optics via the AFOSR award number FA9550-14-1-0040, a Grant-in-Aid for Scientific Research (A), and a grant from the John Templeton Foundation. S.H. was sup-

ported by the NSF (Grant No. PHY-1314861). This work was also supported by the funds of Hangzhou City for supporting the Hangzhou-City Quantum Information and Quantum Optics Innovation Research Team.

APPENDIX A

Derivation of an effective Hamiltonian

Let us start with the originial Hamiltonian given in Eq. (11), i.e.,

$$H = g_a(\hat{a}\sigma_{fg}^{+}e^{i\Delta_a t} + h.c.) + g_b(\hat{b}\sigma_{eg}^{+}e^{i\delta_b t} + h.c.) + \Omega(e^{i\Delta t}\sigma_{fe}^{+} + h.c.), \quad (15)$$

where $\sigma_{eg}^{+} = |e\rangle\langle g|$ and $\sigma_{fg}^{+} = |f\rangle\langle g|$, Ω is the Rabi frequency of the pulse, and $\hat{a}$ ($\hat{b}$) is the photon annihilation operator for quantum oscillator a (b).

Under the large-detuning conditions $\Delta_a \gg g_a$ and $\Omega \gg \Delta$, there is no energy exchange between oscillator a and the coupler, as well as between the pulse and the coupler [Fig. 1(a)]. In addition, under the conditions $\Delta_a - \delta_b \gg g_a g_b \left(\Delta_a^{-1} + \delta_b^{-1}\right)/2$ and $\Delta - \delta_b \gg \Omega g_b \left(\Delta^{-1} + \delta_b^{-1}\right)/2$, there is no interaction between oscillator b and either of oscillator a and the pulse [Fig. 1(a)]. In this case, the effective Hamiltonian can be expressed as [58]

$$\begin{aligned} H_{\rm eff} = {} & \frac{g_a^2}{\Delta_a}[\,|f\rangle\langle f| + \hat{a}^\dagger\hat{a}(|f\rangle\langle f| - |g\rangle\langle g|)\,] \\ & + \frac{\Omega^2}{\Delta}(|f\rangle\langle f| - |e\rangle\langle e|) \\ & - \tilde{g}_a(\hat{a}\sigma_{eg}^{+}e^{i\delta_a t} + h.c.) \\ & + g_b(\hat{b}\sigma_{eg}^{+}e^{i\delta_b t} + h.c.), \end{aligned} \quad (16)$$

where $\tilde{g}_a = g_a\Omega(\Delta_a^{-1} + \Delta^{-1})/2$ and $\delta_a = \Delta_a - \Delta$. Under the large-detuning conditions $\delta_a \gg \{\tilde{g}_a, g_a^2/\Delta_a, \Omega^2/\Delta\}$ and $\delta_b \gg \{g_b, g_a^2/\Delta_a, \Omega^2/\Delta\}$, the effective Hamiltonian $H_{\rm eff}$ becomes [58]

$$\begin{aligned} H_{\rm eff} = {} & \frac{\tilde{g}_a^2}{\delta}[|e\rangle\langle e| + \hat{a}^\dagger\hat{a}(|e\rangle\langle e| - |g\rangle\langle g|)] \\ & + \frac{g_b^2}{\delta_b}[|e\rangle\langle e| + \hat{b}^\dagger\hat{b}(|e\rangle\langle e| - |g\rangle\langle g|)] \\ & + \frac{g_a^2}{\Delta_a}[|f\rangle\langle f| + \hat{a}^\dagger\hat{a}(|f\rangle\langle f| - |g\rangle\langle g|)] \\ & + \frac{\Omega^2}{\Delta}(|f\rangle\langle f| - |e\rangle\langle e|) \\ & - \frac{\tilde{g}_a g_b}{2}\left(\frac{1}{\delta_a} + \frac{1}{\delta_b}\right) \times \\ & [(\hat{a}\hat{b}^\dagger|e\rangle\langle e| - \hat{a}^\dagger\hat{b}|g\rangle\langle g|)e^{i(\delta_a - \delta_b)t} + h.c.]. \end{aligned} \quad (17)$$

When the levels $|e\rangle$ and $|f\rangle$ are not occupied, the effective Hamiltonian $H_{\rm eff}$ reduces to

$$\begin{aligned} H_{eff} = {} & -\left(\frac{g_a^2}{\Delta_a} + \frac{\tilde{g}_a^2}{\delta}\right)\hat{a}^\dagger\hat{a}|g\rangle\langle g| - \frac{g_b^2}{\delta}\hat{b}^\dagger\hat{b}|g\rangle\langle g| \\ & + \lambda(\hat{a}\hat{b}^\dagger + \hat{a}^\dagger\hat{b})|g\rangle\langle g|, \end{aligned} \quad (18)$$

where $\lambda = \tilde{g}_a g_b/\delta$ and we have set $\delta_a = \delta_b = \delta$.

Master equation and parameters used in numerical simulation

After taking dissipation and dephasing into account, the system dynamics is determined by the master equation

$$\begin{aligned} \frac{d\rho}{dt} = {} & -i\left[H', \rho\right] + \kappa_a\mathcal{L}\left[\hat{a}\right] + \kappa_b\mathcal{L}\left[\hat{b}\right] \\ & + \sum_{j=g,g',e}\gamma_{fj}\mathcal{L}\left[\sigma_{fj}^{-}\right] + \sum_{k=g,g'}\gamma_{ek}\mathcal{L}\left[\sigma_{ek}^{-}\right] + \gamma_{g'g}\mathcal{L}\left[\sigma_{g'g}^{-}\right] \\ & + \sum_{j=g',e,f}\gamma_{\varphi,l}\left(\sigma_{ll}\rho\sigma_{ll} - \sigma_{ll}\rho/2 - \rho\sigma_{ll}/2\right), \end{aligned} \quad (19)$$

where $\mathcal{L}\left[\Lambda\right] = \Lambda\rho\Lambda^{+} - \Lambda^{+}\Lambda\rho/2 - \rho\Lambda^{+}\Lambda/2$ (with $\Lambda = \hat{a}, \hat{b}, \sigma_{g'g}^{-}, \sigma_{eg}^{-}, \sigma_{eg'}^{-}, \sigma_{fg}^{-}, \sigma_{fg'}^{-}, \sigma_{fe}^{-}$), $\sigma_{g'g'} = |g'\rangle\langle g'|$, $\sigma_{ee} = |e\rangle\langle e|$, and $\sigma_{ff} = |f\rangle\langle f|$. In addition, κ_a (κ_b) is the decay rate of resonator a (b); $\gamma_{g'g}$, γ_{eg}, $\gamma_{eg'}$, γ_{fg}, $\gamma_{fg'}$ and γ_{fe} are the energy relaxation rates for $|g'\rangle \to |g\rangle$, $|e\rangle \to |g\rangle$, $|e\rangle \to |g'\rangle$, $|f\rangle \to |g\rangle$, $|f\rangle \to |g'\rangle$, and $|f\rangle \to |e\rangle$, respectively; $\gamma_{\varphi,g'}$, $\gamma_{\varphi,e}$, and $\gamma_{\varphi,f}$ are the dephasing rates of the levels $|g'\rangle$, $|e\rangle$, and $|f\rangle$.

The parameters used in the numerical simulation are: (i) $\Delta_a/2\pi = 1.5$ GHz, $\Delta/2\pi = 1.25$ GHz; (ii) $\delta_b/2\pi = 0.25$ GHz; (iii) $\gamma_{\varphi,g'}^{-1} = \gamma_{\varphi,e}^{-1} = \gamma_{\varphi,f}^{-1} = 15$ μs; (iv) $\gamma_{g'g}^{-1} = 60$ μs, $\gamma_{eg'}^{-1} = 40$ μs, $\gamma_{fe}^{-1} = 30$ μs, $\gamma_{eg}^{-1} = \gamma_{fg'}^{-1} = \gamma_{fg}^{-1} = 100$ μs [59]; and (v) $\kappa_a^{-1} = \kappa_a^{-1} = 20$ μs. We choose $g_{12} = 0.1\max\{g_a, g_b\}$. Here we consider a rather conservative case for both the inter-resonator crosstalk and the decoherence time of flux qudits because the inter-resonator crosstalk strength can be smaller by at least one order of magnitude [29] and decoherence time ranging from 70 μs to 1 ms has been reported for a superconducting qudit [60-63].

[1] T. Jennewein, C. Simon, G. Weihs, H. Weinfurter, and A. Zeilinger, Quantum cryptography with entangled photons, Phys. Rev. Lett. **84**, 4729 (2000).

[2] J. Jing, J. Zhang, Y. Yan, F. Zhao, C. Xie, and K. Peng, Experimental demonstration of tripartite entanglement and controlled dense coding for continuous variables, Phys. Rev. Lett. **90**, 167903 (2003).

[3] W. Tittel, H. Zbinden, and N. Gisin, Experimental demonstration of quantum secret sharing, Phys. Rev. A **63**, 042301 (2001).

[4] N. Takei, H. Yonezawa, T. Aoki, and A. Furusawa, High-fidelity teleportation beyond the no-cloning limit and entanglement swapping for continuous variables, Phys. Rev. Lett. **94**, 220502 (2005).

[5] D. Bouwmeester, J. W. Pan, K. Mattle, M. Eibl, H. Weinfurter, and A. Zeilinger, Experimental quantum teleportation, Nature **390**, 575 (1997).

[6] A. Furusawa, J. L. Sørensen, S. L. Braunstein, C. A. Fuchs, H. J. Kimble, and E. S. Polzik, Unconditional quantum teleportation, Science **282**, 706 (1998).

[7] J. Yin, J. G. Ren, H. Lu, Y. Cao, H. L. Yong, Y. P. Wu, C. Liu, S. K. Liao, F. Zhou, and Y. Jiang *et al.*, Quantum teleportation and entanglement distribution over 100-kilometre free-space channels, Nature **488**, 185 (2012).

[8] X. L. Wang, X. D. Cai, Z. E. Su, M. C. Chen, D. Wu, L. Li, N. L. Liu, C. Y. Lu, and J. W. Pan, Quantum teleportation of multiple degrees of freedom of a single photon, Nature **518**, 516 (2015).

[9] Y. F. Huang, B. H. Liu, L. Peng, Y. H. Li, L. Li, C. F. Li, and G. C. Guo, Experimental generation of an eight-photon Greenberger-Horne-Zeilinger state, Nat. Commun. **2**, 546 (2011).

[10] X. C. Yao, T. X. Wang, P. Xu, H. Lu, G. S. Pan, X. H. Bao, C. Z. Peng, C. Y. Lu, Y. A. Chen, and J. W. Pan, Observation of eight-photon entanglement, Nat. Photon. **6**, 225 (2012).

[11] Z. Y. Ou, S. F. Pereira, H. J. Kimble, and K. C. Peng, Realization of the Einstein-Podolsky-Rosen paradox for continuous variables, Phys. Rev. Lett. **68**, 3663 (1992).

[12] Y. Zhang, H. Wang, X. Li, J. Jing, C. Xie, and K. Peng, Experimental generation of bright two-mode quadrature squeezed light from a narrow-band nondegenerate optical parametric amplifier, Phys. Rev. A **62**, 023813 (2000).

[13] A. Ourjoumtsev, F. Ferreyrol, R. Tualle-Brouri, and P. Grangier, Preparation of non-local superpositions of quasi-classical light states, Nat. Phys. **5**, 189 (2009).

[14] T. Eberle, V. Händchen, J. Duhme, T. Franz, R. F. Werner, and R. Schnabel, Strong Einstein-Podolsky-Rosen entanglement from a single squeezed light source, Phys. Rev. A **83**, 052329 (2011).

[15] A. S. Villar, L. S. Cruz, K. N. Cassemiro, M. Martinelli, and P. Nussenzveig, Generation of bright two-color continuous variable entanglement, Phys. Rev. Lett. **95**, 243603 (2005).

[16] A. S. Coelho, F. A. S. Barbosa, K. N. Cassemiro, A. S. Villar, M. Martinelli, and P. Nussenzveig, Three-color entanglement, Science **326**, 823 (2009).

[17] X. Jia, Z. Yan, Z. Duan, X. Su, H. Wang, C. Xie, and K. C. Peng, Experimental realization of three-color entanglement at optical fiber communication and atomic storage wavelengths, Phys. Rev. Lett. **109**, 253604 (2012).

[18] O. Morin, K. Huang, J. Liu, H. L. Jeannic, C. Fabre, and J. Laurat, Remote creation of hybrid entanglement between particle-like and wave-like optical qubits, Nat. Photon. **8**, 570 (2014).

[19] H. Jeong, A. Zavatta, M. Kang, S. W. Lee, L. S. Costanzo, S. Grandi, T. C. Ralph, and M. Bellini, Generation of hybrid entanglement of light, Nat. Photon. **8**, 564 (2014).

[20] M. D. Reid and P. D. Drummond, Quantum correlations of phase in nondegenerate parametric oscillation, Phys. Rev. Lett. **60**, 2731 (1988).

[21] C. C. Gerry, Generation of optical macroscopic quantum superposition states via state reduction with a Mach-Zehnder interferometer containing a Kerr medium, Phys. Rev. A **59**, 4095 (1999).

[22] J. Fiurášek, Conditional generation of N-photon entangled states of light, Phys. Rev. A **65**, 053818 (2002).

[23] H. Xiong, M. O. Scully, and M. S. Zubairy, Correlated spontaneous emission laser as an entanglement amplifier, Phys. Rev. Lett. **94**, 023601 (2005).

[24] S. Pielawa, G. Morigi, D. Vitali, and L. Davidovich, Generation of Einstein-Podolsky-Rosen-entangled radiation through an atomic reservoir, Phys. Rev. Lett. **98**, 240401 (2007).

[25] F. Xue, Y.X. Liu, C.P. Sun, F. Nori, Two-mode squeezed states and entangled states of two mechanical resonators Phys. Rev. B **76**, 064305 (2007).

[26] M. D. Reid, P. D. Drummond, W. P. Bowen, E. G. Cavalcanti, P. K. Lam, H. A. Bachor, U. L. Andersen, and G. Leuchs, Colloquium: the Einstein-Podolsky-Rosen paradox: from concepts to applications, Rev. Mod. Phys. **81**, 1727 (2009).

[27] P. B. Li, S. Y. Gao, and F. L. Li, Engineering two-mode entangled states between two superconducting resonators by dissipation, Phys. Rev. A **86**, 012318 (2012).

[28] S. T. Merkel and F. K. Wilhelm, Generation and detection of NOON states in superconducting circuits, New J. Phys. **12**, 093036 (2010); F. W. Strauch, All-resonant control of superconducting resonators, arXiv:1208.3657.

[29] C. P. Yang, Q. P. Su, and S. Han, Generation of Greenberger-Horne-Zeilinger entangled states of photons in multiple cavities via a superconducting qutrit or an atom through resonant interaction, Phys. Rev. A **86**, 022329 (2012).

[30] C. P. Yang, Q. P. Su, S. B. Zheng, and S. Han, Generating entanglement between microwave photons and qubits in multiple cavities coupled by a superconducting qutrit, Phys. Rev. A **87**, 022320 (2013).

[31] Q. P. Su, C. P. Yang, and S. B. Zheng, Fast and simple scheme for generating NOON states of photons in circuit QED, Sci. Rep. **4**, 3898 (2014).

[32] J. R. Johansson, N. Lambert, I. Mahboob, H. Yamaguchi, F. Nori, Entangled-state generation and Bell inequality violations in nanomechanical resonators, Phys. Rev. B **90**, 174307 (2014).

[33] M. Hua, M. J. Tao, and F. G. Deng, One-step implementation of entanglement generation on microwave photons in distant 1D superconducting resonators, arXiv:1508.00061.

[34] T. P. Purdy, P.-L. Yu, R.W. Peterson, N. S. Kampel, and C. A. Regal, Strong Optomechanical Squeezing of Light, Phys. Rev. X 3, 031012 (2013).

[35] A. H. Safavi-Naeini et al., Squeezed light from a silicon micromechanical resonator, Nature (London) 500, 185 (2013).

[36] L. Tian, Robust Photon Entanglement via Quantum Interference in Optomechanical Interfaces, Phys. Rev. Lett. 110, 233602 (2013).

[37] S. D. Bennett, N. Y. Yao, J. Otterbach, P. Zoller, P. Rabl, and M. D. Lukin, Phonon-Induced Spin-Spin In-

teractions in Diamond Nanostructures: Application to Spin Squeezing, Phys. Rev. Lett. 110, 156402 (2013).

[38] M. Schleier-Smith, Editorial: Hybridizing Quantum Physics and Engineering, Phys. Rev. Lett. 117, 100001 (2016).

[39] G. Drobný, B. Hladký, and V. Bužek, Quantum-state synthesis of multimode bosonic fields: Preparation of arbitrary states of two-dimensional vibrational motion of trapped ions, Phys. Rev. A **58**, 2481 (1998).

[40] F. W. Strauch, K. Jacobs, and R. W. Simmonds, Arbitrary control of entanglement between two superconducting resonators, Phys. Rev. Lett. **105**, 050501 (2010).

[41] F. W. Strauch, D. Onyango, K. Jacobs, and R. W. Simmonds, Entangled-state synthesis for superconducting resonators, Phys. Rev. A **85**, 022335 (2012).

[42] R. Sharma and F. W. Strauch, Quantum state synthesis of superconducting resonators, Phys. Rev. A **93**, 012342 (2016).

[43] Y. J. Zhao, C. Q. Wang, X. Zhu, Y. X. Liu, Engineering entangled microwave photon states via multiphoton transitions between two cavities and a superconducting qubit, arXiv:1506.06363.

[44] N. Ofek, A. Petrenko, R. Heeres, P. Reinhold, Z. Leghtas, B. Vlastakis, Y. Liu, L. Frunzio, S. M. Girvin, L. Jiang, M. Mirrahimi, M. H. Devoret, and R. J. Schoelkopf, Demonstrating quantum error correction that extends the lifetime of quantum information, arXiv:1602.04768.

[45] I. Buluta, S. Ashhab, and F. Nori, Natural and artificial atoms for quantum computation, Rep. Prog. Phys. **74**, 104401 (2011).

[46] J. Q. You and F. Nori, Superconducting circuits and quantum information, Phys. Today **58**, 42 (2005).

[47] J. Clarke and F. K. Wilhelm, Superconducting quantum bits, Nature **453**, 1031 (2008).

[48] J. Q. You and F. Nori, Atomic physics and quantum optics using superconducting circuits, Nature **474**, 589 (2011).

[49] Z. L. Xiang, S. Ashhab, J. Q. You, and F. Nori, Hybrid quantum circuits: Superconducting circuits interacting with other quantum systems, Rev. Mod. Phys. **85**, 623 (2013).

[50] C. P. Yang, Q. P. Su, S. B. Zheng, and F. Nori, Entangling superconducting qubits in a multi-cavity system, New J. Phys. **18**, 013025 (2016).

[51] M. Sandberg, C.M.Wilson, F. Persson, T. Bauch, G. Johansson, V. Shumeiko, T. Duty, and P. Delsing, Tuning the field in a microwave resonator faster than the photon lifetime, Appl. Phys. Lett. **92**, 203501 (2008).

[52] Z. L. Wang, Y. P. Zhong, L. J. He, H. Wang, J. M. Martinis, A. N. Cleland, and Q. W. Xie, Quantum state characterization of a fast tunable superconducting resonator, Appl. Phys. Lett. **102**, 163503 (2013).

[53] T. Niemczyk, F. Deppe, H. Huebl, E. P. Menzel, F. Hocke, M. J. Schwarz, J. J. Garcia-Ripoll, D. Zueco, T. Hüummer, and E. Solano *et al.*, Circuit quantum electrodynamics in the ultrastrong-coupling regime, Nature Phys. **6**, 772 (2010).

[54] F. Yoshihara, Y. Nakamura, F. Yan, S. Gustavsson, J. Bylander, W. D. Oliver, and J. S. Tsai, Flux qubit noise spectroscopy using Rabi oscillations under strong driving conditions, Phys. Rev. B **89**, 020503(R) (2014).

[55] W. Chen, D. A. Bennett, V. Patel, and J. E. Lukens, Substrate and process dependent losses in superconducting thin film resonators, Sci. Technol. **21**, 075013 (2008).

[56] P. J. Leek, M. Baur, J. M. Fink, R. Bianchetti, L. Steffen, S. Filipp, and A. Wallraff, Cavity quantum electrodynamics with separate photon storage and qubit readout modes, Phys. Rev. Lett. **104**, 100504 (2010).

[57] M. D. Reed, L. DiCarlo, B. R. Johnson, L. Sun, D. I. Schuster, L. Frunzio, and R. J. Schoelkopf, High-fidelity readout in circuit quantum electrodynamics using the Jaynes-Cummings nonlinearity, Phys. Rev. Lett. **105**, 173601 (2010).

[58] D. F. V. James and J. Jerke, Effective Hamiltonian theory and its applications in quantum information, Can. J. Phys. **85**, 625 (2007).

[59] By designing the flux qudit, the $|e\rangle \leftrightarrow |g\rangle$, $|f\rangle \leftrightarrow |g'\rangle$, and $|f\rangle \leftrightarrow |g\rangle$ dipole matrix elements can be made much smaller than those of the $|g'\rangle \leftrightarrow |g\rangle$, $|e\rangle \leftrightarrow |g'\rangle$, and $|f\rangle \leftrightarrow |e\rangle$ transitions. Thus, $\gamma_{eg}^{-1}, \gamma_{fg'}^{-1}, \gamma_{fg}^{-1} \gg \gamma_{g'g}^{-1}, \gamma_{eg'}^{-1}, \gamma_{fe}^{-1}$.

[60] F. Yan, S. Gustavsson, A. Kamal, J. Birenbaum, A. P. Sears, D. Hover, T. J. Gudmundsen, J. L. Yoder, T. P. Orlando, and J. Clarke *et al.*, The Flux Qubit Revisited, arXiv:1508.06299; J. Q. You, X. Hu, S. Ashhab, and F. Nori, Low-decoherence flux qubit, Phys. Rev. B **75**, 140515(R) (2007).

[61] M. J. Peterer, S. J. Bader, X. Jin, F. Yan, A. Kamal, T. J. Gudmundsen, P. J. Leek, T. P. Orlando, W. D. Oliver, and S. Gustavsson, Coherence and decay of higher energy levels of a superconducting transmon qubit, Phys. Rev. Lett. **114**, 010501 (2015).

[62] C. Rigetti, J. M. Gambetta, S. Poletto, B. L. T. Plourde, J. M. Chow, A. D. Córcoles, J. A. Smolin, S. T. Merkel, J. R. Rozen, and G. A. Keefe *et al.*, Superconducting qubit in a waveguide cavity with a coherence time approaching 0.1 ms, Phys. Rev. B **86**, 100506(R) (2012).

[63] I. M. Pop, K. Geerlings, G. Catelani, R. J. Schoelkopf, L. I. Glazman, and M. H. Devoret, Coherent suppression of electromagnetic dissipation due to superconducting quasiparticles, Nature **508**, 369 (2014).